CMS Physics Analysis Summary

Contact: cms-pag-conveners-smp@cern.ch 2013/07/24

Measurement of the WZ production cross section in the $\ell^+\ell^-\ell'\nu$ decay channel at $\sqrt{s} = 7$ and 8 TeV at the LHC

The CMS Collaboration

Abstract

This note presents measurements of WZ production in proton-proton collisions at center of mass energies of 7 TeV and 8 TeV with the CMS experiment at the Large Hadron Collider. Results are based on data corresponding to integrated luminosities of 4.9 fb^{-1} collected at $\sqrt{s} = 7$ TeV, and 19.6 fb^{-1} collected at $\sqrt{s} = 8$ TeV. The leptonic decay modes of the W and Z bosons into electrons and muons are considered. The inclusive WZ cross section is determined for the two energies, and the ratio of production cross sections for W^+Z and W^-Z is determined.

1 Introduction

The study of diboson production in proton-proton collisions represents an important test of the standard model (SM) because of its sensitivity to the self-interaction between gauge bosons via trilinear gauge couplings (TGC). These couplings are a direct consequence of the non-Abelian $SU(2) \times U(1)$ gauge symmetry of the SM and are a necessary ingredient to construct renormalizable theories with massive gauge bosons. In the SM, two processes contribute to WZ production in hadron collisions at leading order in α_s, and both involve an incoming quark and antiquark: the W and Z bosons can be directly radiated from the initial incoming quark and antiquark (t and u channel), or the Z boson can be radiated from a W boson produced through quark-antiquark annihilation (s channel) through the WWZ vertex. WZ production has been previously observed in hadron collisions at the Tevatron [1, 2], and at the LHC by both ATLAS [3, 4] and CMS [5].

This note presents measurements of the WZ production cross section using data collected in 2011 and 2012 by the Compact Muon Solenoid (CMS) experiment at the Large Hadron Collider (LHC) at center of mass energies of 7 TeV and 8 TeV. The data correspond to integrated luminosities of 4.9 fb^{-1} at 7 TeV and 19.6 fb^{-1} at 8 TeV. The purely leptonic final states containing electrons and muons are used in these measurements. Beyond the standard model (BSM) signals decaying via WZ to final states with electrons and muons have already been searched for using this data[6]. The results presented in this note supersede the previous CMS measurement [5], which was based on 1.09 fb^{-1} of data collected at $\sqrt{s} = 7$ TeV. Besides using more data, these measurements represent an improvement over that first measurement by using improved lepton identification and by following a more general approach in the determination of the fake lepton background.

2 Data samples and simulation

A detailed description of the CMS detector can be found elsewhere [7]. The layout comprises a superconducting solenoid providing a uniform magnetic field of 3.8 T. The bore of the solenoid is instrumented with various particle detection systems. The inner tracking system is composed of a pixel detector with three barrel layers at radii between 4.4 and 10.2 cm and a silicon strip tracker with 10 barrel detection layers extending outwards to a radius of 1.1 m. Each system is completed by two end caps, extending the acceptance up to $|\eta| < 2.5$. A lead tungstate crystal electromagnetic calorimeter (ECAL) with fine transverse $(\Delta\eta, \Delta\phi)$ granularity and a brass-scintillator hadronic calorimeter surround the tracking volume and cover the region $|\eta| < 3$. The steel return yoke outside the solenoid is in turn instrumented with gas detectors which are used to identify muons in the range $|\eta| < 2.4$. The barrel region is covered by drift tube chambers (DT) and the end cap region by cathode strip chambers (CSC), each complemented by resistive plate chambers (RPC).

Events for these measurements are selected using triggers which require the presence of two leptons, be it electrons or muons. For the analysis of 7 TeV data only double electron or double muons triggers are used, while triggers requiring the presence of an electron and a muon are also used for the analysis of 8 TeV data.

A number of Monte Carlo event generators are used to simulate the signal and backgrounds. The WZ signal, W+jets, Z+jets, $\text{t}\bar{\text{t}}$, WW, $\text{Z}\gamma$ processes are generated using the MADGRAPH [8] event generator. The W+jets process has been found not to contribute to the selected event sample in this measurement and will therefore not be further discussed. The POWHEG program [9] was used to generate ZZ processes. For leading-order generators, the default set of parton dis-

tribution functions (PDF) used to produce these samples is CTEQ6L [10], while CT10 [11] is used for next-to-leading order generators. NLO calculations are used for background cross sections. For all processes, the detector response is simulated using a detailed description of the CMS detector, based on the GEANT4 package [12].

The simulated samples are reweighted in order to reproduce the distribution of the number of pp interactions per bunch crossing (pile-up) observed in data.

3 Event selection

The fully leptonic WZ final states are studied, considering the four final states with electrons and muons: eee, eeμ, $\mu\mu$e and $\mu\mu\mu$. This measurement relies therefore on a good identification of electrons and muons, and on a good measurement of the missing transverse energy.

3.1 Lepton identification

Muon candidates [13] are identified using a selection close to the one described in Ref. [14], while electron candidates are selected in the same way as in the $H \to W^+W^- \to \ell\nu\ell\nu$ analyses, using a multivariate approach, which exploits correlations between the selection variables described in [15] to improve identification performance. The lepton candidates are required to be compatible with the primary vertex of the event, which is chosen as the vertex with highest $\sum p_T^2$ of its associated tracks. This criterion provides the correct assignment for the primary vertex in more than 99% of both signal and background events for the pile-up distribution observed in the data.

Leptons from W and Z decays will tend to be isolated from other particles in the event, while hadrons misidentified as leptons or leptons from heavy quark decays will usually be close to a jet. Requiring leptons to be isolated from other final state particles is therefore a powerful way to discriminate against such background leptons and several isolation variables are defined to achieve this. For each lepton candidate, a cone is constructed around the track direction at the event vertex. The scalar sum of the transverse energy of each reconstructed particle [16] compatible with the chosen primary vertex and contained within the cone is calculated excluding the contribution from the lepton candidate itself. If this sum exceeds approximately 10% of the candidate p_T the lepton is rejected – the exact requirement depending on the lepton η, p_T and flavor. Lepton reconstruction, identification and isolation efficiencies are measured directly in data using the "Tag-and-Probe" method [17]. The measured energy in the cone is corrected for the contribution from pile-up events.

Neutrinos from leptonic W boson decays do not interact with the detector and result in a significant missing transverse energy, E_T^{miss}, in the event. The E_T^{miss} in these analyses is calculated with the particle-flow method [18]. The algorithm combines information from the tracking system, the muon chambers, and from all the calorimetry to classify reconstructed objects according to their particle type (electron, muon, photon, charged or neutral hadron). This allows precise corrections to particle energies and also provides a significant degree of redundancy, which renders the E_T^{miss} measurement less sensitive to calorimetry miscalibration. The E_T^{miss} is computed as the magnitude of the negative vector sum of transverse energies of all particle-flow objects.

3.2 Analysis selection

The $WZ \to 3\ell$ decay is characterized by a pair of same-flavor, opposite-charge, isolated leptons with an invariant mass corresponding to a Z boson, together with a third isolated lepton and

a significant amount of missing transverse energy associated to the escaping neutrino. The same selection has essentially been applied to the 2011 and 2012 datasets. Differences will be indicated where present.

Candidate events are required to have fired a di-electron or di-muon trigger for final states with Z decaying into electrons or muons, respectively. In the 8 TeV analysis events that have fired the electron-muon trigger are also accepted. The leptons used to reconstruct the Z decay must satisfy the trigger requirements. Selected events are required to contain only 3 leptons, electrons or muons, matching all selection criteria.

Z candidates are built from two opposite-sign same-flavour leptons passing the electron or muon identification criteria. The leading and second leading lepton are required to have $p_{\mathrm{T}} > 20$ GeV and $p_{\mathrm{T}} > 10$ GeV, respectively. The Z candidate invariant mass should lie within 20 GeV of the nominal Z mass. In case several matching pairs are found, the Z candidate with the mass closest to the nominal Z mass is selected. The remaining lepton is associated to the W boson decay. It is required to have $p_{\mathrm{T}} > 20$ GeV. Finally, the missing transverse energy in the event is required to be larger than 30 GeV to select W boson decays. This requirement discriminates against jets faking leptons or photon conversions from Z+jets or Zγ events.

4 Background determination

The background sources come from events with three leptons, genuine or fake, and can be grouped into three classes: non-peaking background, Z+fake lepton background, and Z+prompt lepton background. Examples of non-peaking backgrounds are tt, QCD multijet, and W+jets production; all but the first of these can be neglected in this analysis. Z+fake lepton backgrounds are the most important for the WZ $\to 3\ell$ process; they include fake or non-isolated leptons from jets (including heavy quark jets) or photons. Z+prompt lepton backgrounds originate primarily from the ZZ $\to 4\ell$ process, where one of the four leptons is lost; it is irreducible but small due to the reduced ZZ production cross section.

4.1 Determination of the fake lepton background

4.1.1 Method description

To estimate the fake lepton background, we follow the general fakeable object method used in [14]. The method uses the definition of a looser lepton identification, in which some of the lepton identification requirements used in the final lepton selection are relaxed. We distinguish lepton categories according to their real origin:

- *prompt leptons*: they are real leptons originating from heavy boson decays. They are usually isolated from other particles in the event.
- *fake leptons*: they are leptons in jets or hadrons misidentified as leptons.

In the following, we will use the index j (for jets) to denominate fake leptons, while we use the index ℓ (for leptons) to denominate prompt leptons, and we order the 3 leptons in the WZ final state: W lepton, Z leading lepton and Z trailing lepton. The final sample has contributions from the following event categories:

- $\ell\ell\ell$: the three leptons originate from prompt leptons. Real signal (WZ) events will contribute to this category, as well as irreducible backgrounds with 3 prompt leptons, mostly from ZZ.
- $j\ell\ell$: this category is mostly composed of Z+jets and $\mathrm{t\bar{t}}$ events, in which the two Z

leptons are prompt leptons, while the lepton associated to the W decay is a fake lepton.

- $\ell\ell j$ and $\ell j\ell$: this category is again composed of $t\bar{t}$ and Z+jets events, in which one of the two Z leptons is combined with a fake lepton to form a Z, while the other Z lepton can be associated to the W decay.
- $jj\ell$, $j\ell j$, ℓjj, jjj: two or all three identified leptons are fake leptons. Several processes may contribute to this category: W+jets, Z+jets (in which one or both leptons are lost), $t\bar{t}$ (with fully hadronic top decays), or QCD. Their contribution to the total selected yield can however be neglected.

Given some loose lepton selection, we furthermore distinguish leptons *passing* or *failing* a tighter selection. We define then the following probabilities:

- ϵ_i is the probability for a prompt lepton that passed the loose selection for the i-th lepton to also pass the tight selection;
- p_i is the probability for a fake lepton that passed the loose selection for the i-th lepton to also pass the tight selection.

where the meaning of the index i is:

- $i = 1$: W lepton;
- $i = 2$: Z leading lepton;
- $i = 3$: Z trailing lepton.

We start from a sample in which all three leptons are passing the loose selection. This sample can be decomposed in different contributions according to the origin of the selected leptons:

$$N_{LLL} = n_{\ell\ell\ell} + n_{\ell\ell j} + n_{\ell j\ell} + n_{\ell jj} + n_{j\ell\ell} + n_{j\ell j} + n_{jj\ell} + n_{jjj} \tag{1}$$

This sample can then be split in subsamples depending on whether each of the three leptons passes or fails the tight cut. The number of events in each subsample is labeled N_{ijk} with $i, j, k = T, F$ where T indicates leptons passing the tight selection and F stands for leptons failing the tight selection. The number of events in each category can be expressed as the function of the fake rates and efficiencies p_i and ϵ_i. For instance, the number of events with 3 leptons passing the tight lepton selection can be written as:

$$\begin{aligned} N_{TTT} = & \quad n_{\ell\ell\ell}\epsilon_1\epsilon_2\epsilon_3 + n_{\ell\ell j}\epsilon_1\epsilon_2 p_3 + n_{\ell j\ell}\epsilon_1 p_2\epsilon_3 + n_{\ell jj}\epsilon_1 p_2 p_3 \\ & + \quad n_{j\ell\ell}p_1\epsilon_2\epsilon_3 + n_{j\ell j}p_1\epsilon_2 p_3 + n_{jj\ell}p_1 p_2\epsilon_3 + n_{jjj}p_1 p_2 p_3 \end{aligned} \tag{2}$$

Expressions for event yields N_{TTF}, N_{TFT}, N_{TFF}, N_{FTT}, N_{FTF}, N_{FFF} can be obtained in a similar way, resulting in a set of linear equations. The number of signal events, i.e., events with three

prompt leptons, can be then extracted by solving this set of equations:

$$
\begin{aligned}
n_{\ell\ell\ell} \;=\; & \frac{1}{(\epsilon_1 - p_1)(\epsilon_2 - p_2)(\epsilon_3 - p_3)} \\
& [\; N_{TTT}(1-p_1)(1-p_2)(1-p_3) \\
& -N_{TTF}(1-p_1)(1-p_2)(\;p_3) \\
& -N_{TFT}(1-p_1)(\;p_2)(1-p_3) \\
& +N_{TFF}(1-p_1)(\;p_2)(\;p_3) \\
& -N_{FTT}(\;p_1)(1-p_2)(1-p_3) \\
& +N_{FTF}(\;p_1)(1-p_2)(\;p_3) \\
& +N_{FFT}(\;p_1)(\;p_2)(1-p_3) \\
& -N_{FFF}(\;p_1)(\;p_2)(\;p_3)] \qquad (3)
\end{aligned}
$$

The coefficients for the numbers of events in each category N_{ijk} in equation (3) define the weights to be applied to each event depending on the category to which it belongs. The fake rate and efficiencies p_i and ϵ_i are determined from independent samples. In the following subsections, we define the loose and tight selections for electrons and muons, we describe the determination of the fake rates and efficiencies, and we present the results of the method application to the WZ analysis.

4.1.2 Loose and tight lepton definition

The loose leptons are defined with the same criteria as in the main analysis, but by relaxing some of the selection requirements described in Section 3.1. For muons, the relative isolation cut is relaxed with respect to the tight selection in the loose selection. For electrons, the relative isolation and MVA ID requirements are not applied.

4.1.3 Lepton efficiencies and fake rates

The prompt efficiencies ϵ_i, or ratios of prompt leptons passing the tight criteria over prompt leptons passing the loose criteria, are determined from a $Z \to \ell\ell$ sample using the "Tag-and-Probe" method. It is determined separately for several bins in p_T and η of the leptons. The jet fake rates p_i are taken from a QCD jet enriched sample, using the same procedure applied in the WW cross section measurement [14].

4.1.4 Estimation of fake lepton background

The method outlined in the previous sections was used to determine the number of events with three prompt leptons in the sample passing the full WZ selection. This corresponds to determining $\epsilon_1\epsilon_2\epsilon_3 n_{\ell\ell\ell}$ using equation (3). The results are given for the four studied final states in Table 2 for the 7 TeV analysis, and in Table 3 for 8 TeV data.

4.2 Other backgrounds

After subtracting the contribution from fake leptons, the remaining background receives mainly small contributions from the irreducible ZZ background and from the $Z\gamma$ process, in which the photon is misidentified as an electron. The contribution of these processes to the final selected WZ sample is estimated from simulations.

5 Systematic uncertainties

Systematic uncertainties can be grouped into several categories. In the first group, we combine the uncertainties that affect the product of the acceptance, reconstruction, and identification efficiencies of final state objects, as determined from Monte Carlo simulation. These include uncertainties on lepton and $E_{\mathrm{T}}^{\mathrm{miss}}$ energy scales and resolution, uncertainties on the pile-up modeling in Monte Carlo, as well as theoretical uncertainties in the parton distribution functions (PDFs), renormalization and factorization scales. The second group includes the systematic uncertainties affecting the data vs. simulation correction factors for the efficiencies of the reconstruction and identification requirements. These include lepton reconstruction and identification efficiencies. The lepton efficiencies are determined by the "Tag-and-Probe" method [17] in the same way for data and simulation, and the uncertainty on the ratio of efficiencies is taken as a systematic uncertainty. The third category comprises uncertainties on the background yield. These are dominated by the uncertainties on the data-driven Z+jets and $\mathrm{t\bar{t}}$ background estimation described in Section 4.1. To estimate this uncertainty, we varied the jet E_{T} threshold used to select the QCD jet enriched samples from which the lepton fake rates were estimated. Uncertainties on the ZZ and Zγ cross sections are also considered. As the ZZ cross section has been measured by CMS at both 7 and 8 TeV [19, 20], and the Zγ cross section has been measured at 7 TeV [21], the uncertainty on these measured cross sections were taken. As there is no available measurement of the Zγ measurement at 8 TeV, the uncertainty on the 7 TeV measurment increased by a factor of 2 was assumed. Finally, an additional uncertainty due to the measurement of the integrated luminosity is considered. This uncertainty is 2.2% for 2011 data and 4.4% for 2012 data. A summary of all systematic uncertainties is given in Table 1 for the measurement at 7 and 8 TeV.

Table 1: Summary of systematic uncertainties, in units of percent, in the WZ cross section measurement at 7 TeV and 8 TeV.

	7 TeV					8 TeV				
source	input	eee	eeμ	$\mu\mu$e	$\mu\mu\mu$	input	eee	eeμ	$\mu\mu$e	$\mu\mu\mu$
QCD scale	1.3	1.3	1.3	1.3	1.3	1.6	1.6	1.6	1.6	1.6
PDFs	1.4	1.4	1.4	1.4	1.4	1.4	1.4	1.4	1.4	1.4
lepton and trigger efficiency	–	2.9	2.7	2.0	1.4	1	1.8	1.8	1.8	1.8
$E_{\mathrm{T}}^{\mathrm{miss}}$	–	3.7	3.4	4.3	3.7	1.5 (μ), 2.5 (e), 5 (jets)	2.9	2.9	3.5	3.1
muon momentum scale	1	–	0.60	0.43	1.06	0.2	0.0	0.4	0.9	1.1
electron energy scale	2 (EB), 5 (EE)	1.9	0.75	1.2	–	$f(p_{\mathrm{T}},\eta)$	0.8	0.6	0.1	0.0
pile-up	5	0.27	0.50	1.00	0.64	–	0.8	1.1	0.6	0.9
ZZ cross section	14	0.50	0.92	0.62	0.85	15	0.2	0.2	0.2	0.2
Zγ cross section	7	0	0	0.04	0	15	0.2	0.0	0.2	0.0
data-driven	–	2.7	6.5	6.3	6.0	–	2.7	1.9	2.7	2.6
backgrounds	–	0.2	0.2	0.9	0.2	–	0.8	1.2	1.1	1.0
statistical	–	13.5	13.9	13.1	11.0	–	7.3	6.8	6.0	5.0
systematic	–	6.1	7.8	8.1	7.2	–	4.7	4.4	5.1	4.7
luminosity	2.2	2.2	2.2	2.2	2.2	4.4	4.4	4.4	4.4	4.4

6 Results

6.1 Measured and estimated yields

After applying the full selection, 293 events are selected in the 7 TeV data with 4.9 fb^{-1} of integrated luminosity, while 1480 events are selected in the data at 8 TeV with 19.6 fb^{-1}. The data yield for each channel together with the MC expectation for the different processes is given in Tables 2 and 3 for 7 TeV and 8 TeV data, respectively. The distributions of several kinematic variables for selected events are shown in Figure 1 for the 7 TeV dataset, and in Figure 2 for the data at 8 TeV.

Table 2: Yields of selected events in data at 7 TeV, together with the expected yields from the simulation of various background processes. Numbers correspond to an integrated luminosity of 4.9 fb^{-1} and the corresponding errors are statistical only. The contribution from fake leptons, obtained with the data-driven method described in Section 4.1 is also given. The WV and VVV sets of samples listed in Table 3 are only considered at 8 TeV, as they are negligible for the 7 TeV luminosity.

sample	eee	eeμ	$\mu\mu$e	$\mu\mu\mu$
Z+jets	1.2 ± 0.8	1.2 ± 0.9	0.8 ± 0.6	0.6 ± 0.6
top	0.3 ± 0.1	0.6 ± 0.1	0.6 ± 0.1	1.0 ± 0.1
ZZ	2.0 ± 0.1	3.5 ± 0.1	2.7 ± 0.1	5.1 ± 0.1
Vγ	0	0	0.5 ± 0.5	0
WW	0	0	0	0
WZ	44.7 ± 0.5	49.8 ± 0.5	56.0 ± 0.5	73.8 ± 0.6
total MC	48.2 ± 1.0	55.0 ± 1.0	60.5 ± 1.1	80.5 ± 0.9
data-driven	2.2 ± 0.4	1.5 ± 0.3	2.4 ± 0.4	1.8 ± 0.2
data	64	62	70	97

Table 3: Yields of selected events in data at 8 TeV, together with the expected yields from the simulation of various background processes. Numbers correspond to an integrated luminosity of 19.6 fb^{-1}. The contribution from fake leptons, obtained with the data-driven method described in Section 4.1 is also given. The so-called WV sample contains the following SM processes: W$\gamma^* \to \ell\nu ee$, W$\gamma^* \to \ell\nu\mu\mu$, W$\gamma^* \to \ell\nu\tau\tau$, W$\gamma \to \ell\nu\gamma$, WW, WZ $\to q\bar{q}'\ell\ell$ and WZ $\to \ell\nu q\bar{q}$. In the case of the VVV sample, the SM process considered are WZZ, ZZZ, WWZ, WWW, $t\bar{t}$W, $t\bar{t}$Z, $t\bar{t}$WW, $t\bar{t}\gamma$ and WWγ.

sample	eee	eeμ	$\mu\mu$e	$\mu\mu\mu$
Z+jets	9.8 ± 4.4	16.9 ± 6.0	14.5 ± 5.4	13.8 ± 4.5
top	1.4 ± 0.4	2.7 ± 0.3	6.2 ± 0.7	9.1 ± 1.0
ZZ	2.4 ± 0.1	3.1 ± 0.1	3.9 ± 0.1	5.8 ± 0.1
Zγ	2.4 ± 0.9	0.4 ± 0.4	3.8 ± 1.2	0
WV	0.1 ± 0.1	0.1 ± 0.1	0.2 ± 0.1	2.2 ± 0.7
VVV	6.1 ± 0.3	7.9 ± 0.3	10.4 ± 0.4	13.4 ± 0.4
WZ	193.9 ± 1.4	245.8 ± 1.6	315.9 ± 1.9	428.0 ± 2.2
total MC	216.0 ± 4.7	277.0 ± 6.3	354.9 ± 6.0	472.3 ± 5.2
data-driven	14.8 ± 1.4	27.1 ± 2.9	47.9 ± 3.4	59.0 ± 4.6
data	235	288	400	557

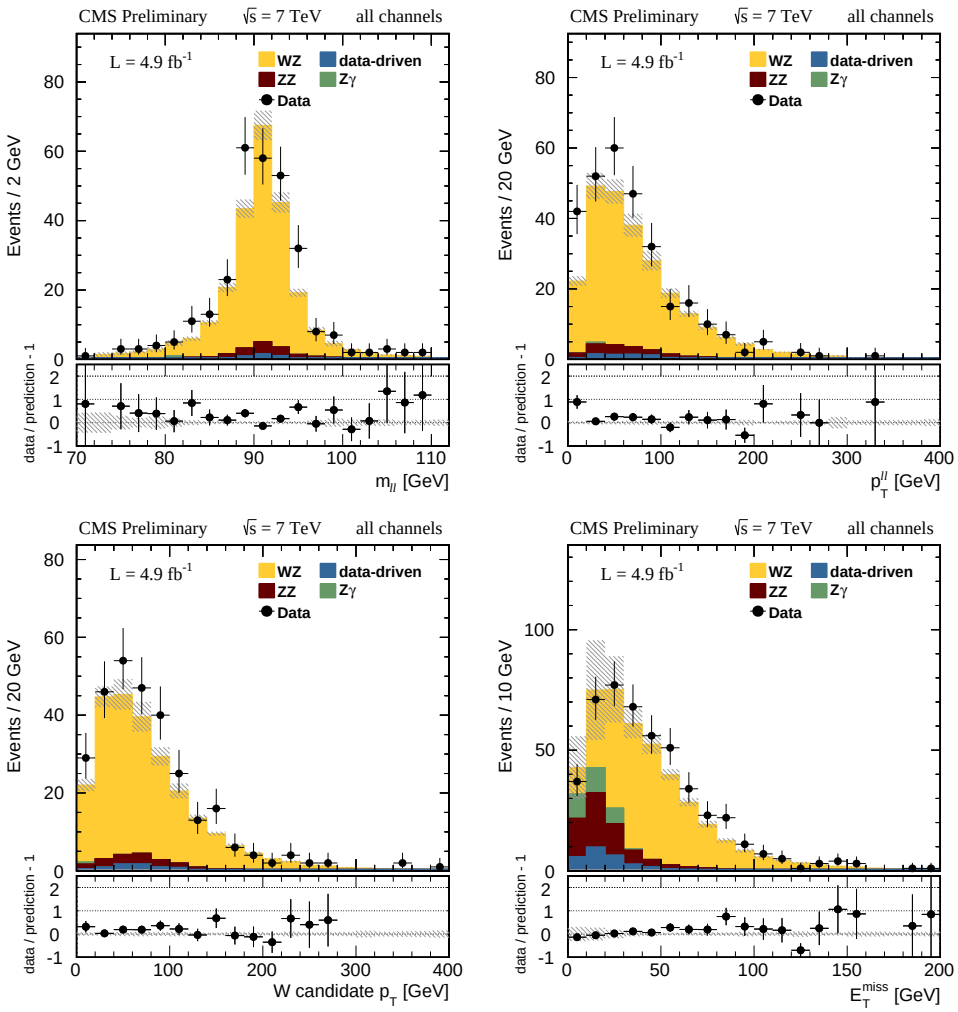

Figure 1: Kinematic distributions after applying all of the WZ selection criteria in the four channels: invariant mass of the Z candidate (top left), transverse momentum of the Z candidate (top right), transverse momentum of the W candidate (bottom left), and the $E_{\mathrm{T}}^{\mathrm{miss}}$ of the event before applying the $E_{\mathrm{T}}^{\mathrm{miss}}$ cut (bottom right), for 7 TeV data. The top and Z+jets backgrounds are estimated using the data-driven method described in the text.

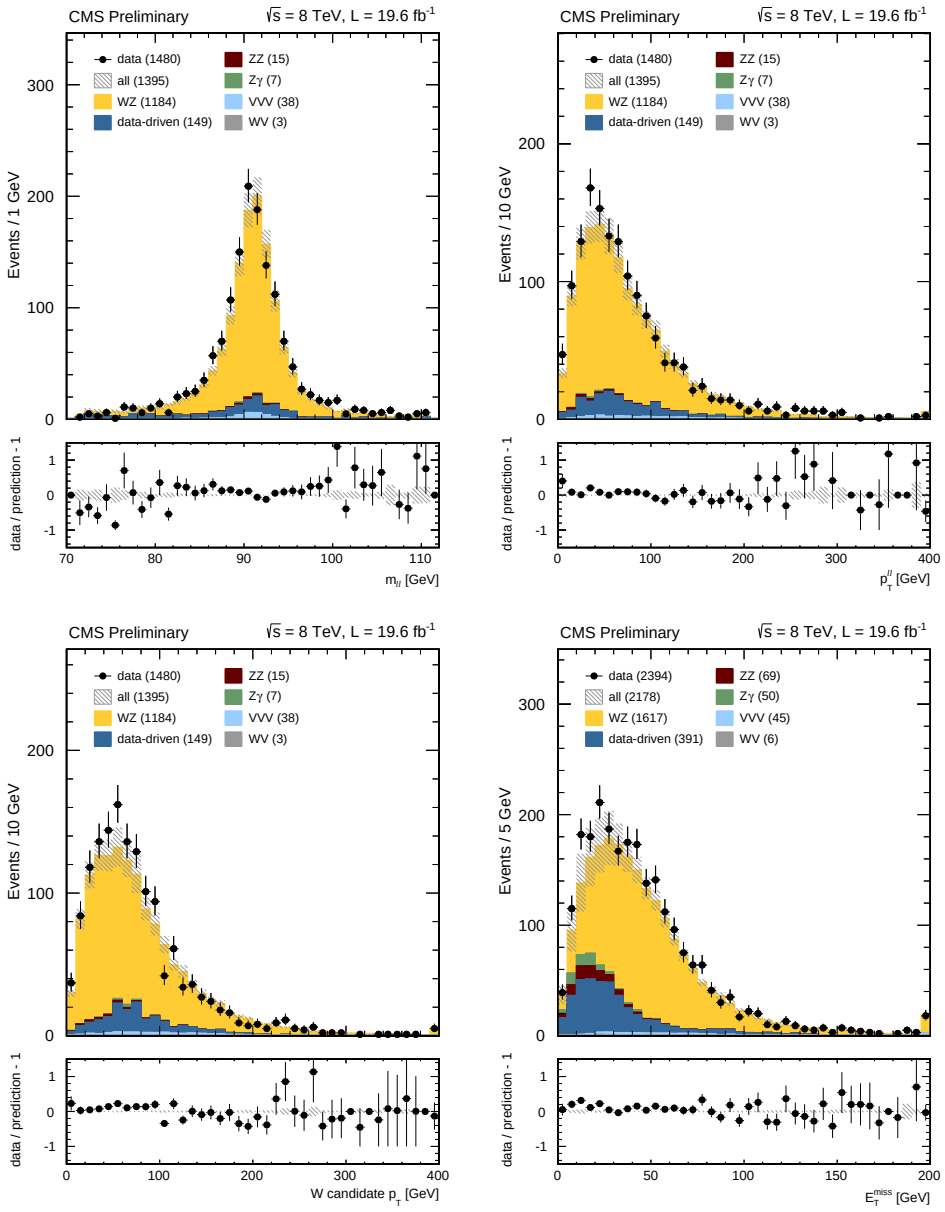

Figure 2: Kinematic distributions after applying all of the WZ selection criteria in the four channels: invariant mass of the Z candidate (top left), transverse momentum of the Z candidate (top right), transverse momentum of the W candidate (bottom left), and the $E_{\mathrm{T}}^{\mathrm{miss}}$ of the event before applying the $E_{\mathrm{T}}^{\mathrm{miss}}$ cut (bottom right), for 8 TeV data. The top and Z+jets backgrounds are estimated using the data-driven method described in the text.

6.2 Measurement of WZ cross section at $\sqrt{s} = 7$ TeV

The cross section is estimated with the expression,

$$\sigma = \frac{N_{\text{sig}}}{A \cdot \epsilon \cdot \mathcal{L}} \tag{4}$$

where N_{sig} is the number of observed signal events, A is the fiducial and kinematic acceptance, ϵ is the selection efficiency for events in the acceptance, and $\mathcal{L}$ is the integrated luminosity. The product $(A \cdot \epsilon)$ is obtained from a simulated WZ sample by determining the fraction of generated WZ events with $71 < m_Z < 111$ GeV that are accepted by the full selection described in Section 3. To account for the difference in trigger, reconstruction and identification efficiencies between data and simulation, each selected simulated event is weighted with an appropriate correction factor. The observed signal yield N_{sig} is obtained by subtracting the estimated backgrounds, described in Section 4, from the number of observed events passing all selection requirements. The inclusive WZ cross section is then measured in four channels. The resulting cross section values are reported in Table 4.

Table 4: Measured WZ cross section values in the four leptonic channels at $\sqrt{s} = 7$ TeV.

channel	$\sigma\left(\text{pp} \to \text{WZ}; \sqrt{s} = 7 \text{ TeV}\right)$ (pb)
eee	23.00 ± 3.10 (stat.) ± 1.39 (syst.) ± 0.51 (lumi.)
eeμ	19.67 ± 2.73 (stat.) ± 1.50 (syst.) ± 0.43 (lumi.)
$\mu\mu$e	19.81 ± 2.60 (stat.) ± 1.55 (syst.) ± 0.44 (lumi.)
$\mu\mu\mu$	21.02 ± 2.30 (stat.) ± 1.47 (syst.) ± 0.46 (lumi.)
combined	20.76 ± 1.32 (stat.) ± 1.13 (syst.) ± 0.46 (lumi.)

We have obtained a combined cross section measurement taking into account the correlation in the uncertainties using the *Best Linear Unbiased Estimator* (BLUE) method [22]. We have assumed full correlation between channel measurements[1] in all uncertainties described in section 5 but for the fakeable object method systematic. Combining the four channels, the total WZ cross section for $71 < m_Z < 111$ GeV is measured to be:

$$\sigma\left(\text{pp} \to \text{WZ} + \text{X}\right) = 20.76 \pm 1.32\ (\text{stat.}) \pm 1.13\ (\text{syst.}) \pm 0.46\ (\text{lumi.})\ \text{pb}$$

The ratio of the inclusive cross-section for individual channels and for the combination to the theoretical NLO prediction of $17.8^{+0.7}_{-0.5}$ pb computed with MCFM [23] using the MSTW2008 PDF set [24], is shown in Figure 3.

6.3 Measurement of WZ cross section at $\sqrt{s} = 8$ TeV

The cross section is extracted in the same way as described above for the 8 TeV data. The measured values for the inclusive WZ cross-section in the four channels are reported in Table 5. The combined total WZ cross section, for $71 < m_Z < 111$ GeV, is measured to be

$$\sigma\left(\text{pp} \to \text{WZ} + \text{X}\right) = 24.61 \pm 0.76\ (\text{stat.}) \pm 1.13\ (\text{syst.}) \pm 1.08\ (\text{lumi.})\ \text{pb}.$$

The theoretical prediction for the WZ production cross section, for a Z boson in the mass range between 71 and 111 GeV, calculated at next-to-leading order in QCD (NLO) using MCFM

[1] Note that some uncertainties are affecting exclusively some channels, for instance electron energy scale are considered to be correlated between the electron content channels.

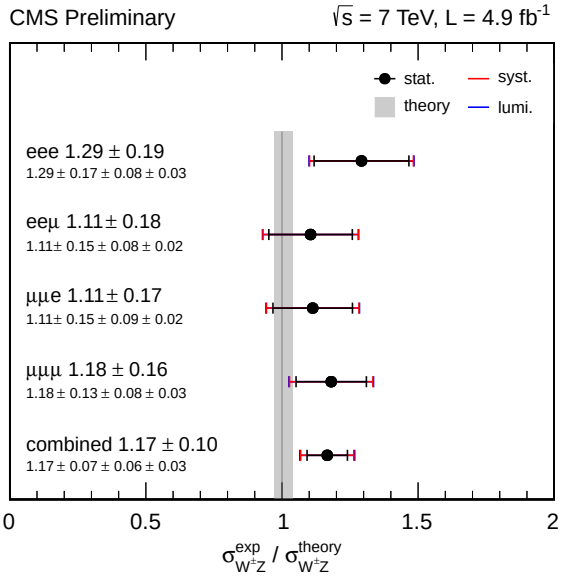

Figure 3: Ratio of measured inclusive cross-section to the theoretical prediction $\sigma_{WZ}^{theo} = 17.8$ pb for WZ production at $\sqrt{s} = 7$ TeV.

6.6 [23] with the MSTW [24] NLO parton density function (PDF) set, is found to be $21.91^{+1.17}_{-0.88}$ pb. The ratio of the inclusive cross sections for individual channels and for the combination to the theoretical NLO prediction is shown in Figure 4.

Table 5: Measured WZ cross section values in the four studied channels at $\sqrt{s} = 8$ TeV.

channel	$\sigma\,(pp \to WZ; \sqrt{s} = 8\ TeV)$ [pb]
eee	24.92 ± 1.83 (stat.) ± 1.25 (syst.) ± 1.10 (lumi.)
eeμ	23.42 ± 1.59 (stat.) ± 1.11 (syst.) ± 1.03 (lumi.)
$\mu\mu$e	24.40 ± 1.46 (stat.) ± 1.33 (syst.) ± 1.07 (lumi.)
$\mu\mu\mu$	25.71 ± 1.27 (stat.) ± 1.34 (syst.) ± 1.13 (lumi.)
combined	24.61 ± 0.76 (stat.) ± 1.13 (syst.) ± 1.08 (lumi.)

6.4 W^+Z/W^-Z ratio measurement

Since the LHC is a proton-proton collider, the W^+Z and W^-Z cross sections are not equal, hence an overall excess of W^+Z events over W^-Z is expected. The ratio of the inclusive cross sections W^+Z and W^-Z is also measured,

$$\frac{\sigma_{W^+Z}}{\sigma_{W^-Z}} = \frac{N_S^+}{N_S^-} \cdot \frac{(\mathcal{A}\cdot\varepsilon)^-}{(\mathcal{A}\cdot\varepsilon)^+} \tag{5}$$

The above equation 5 has been derived from equation 4, where the luminosity is canceled. The lepton and trigger efficiencies ratios of negative to positive leptons, $\varepsilon^-/\varepsilon^+$, have been measured in several CMS's W charge asymmetry analyses [25] and [26], all of them reporting an efficiency ratio compatible with unity within the statistical uncertainty, being 3% for electrons and 2.3% for muons[2]. Nevertheless, the cancellation is valid only in small pseudorapidity bins

[2]The reported uncertainties are shown in η bins. We have chosen the most conservative approach by taking the highest uncertainty value in the binned uncertainties.

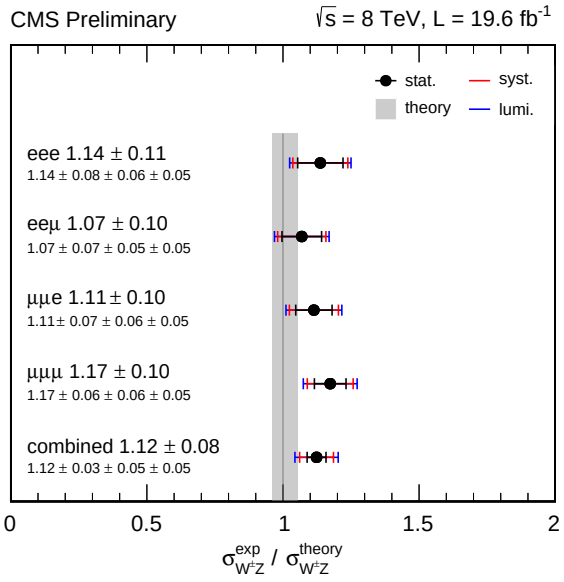

Figure 4: Ratio of measured inclusive cross sections to the theoretical prediction $\sigma_{WZ}^{theo} = 21.91$ pb for WZ production at $\sqrt{s} = 8$ TeV.

and cannot be used in this η integrated measurement. The charge misidentification rate has been found negligible for muons [27], less than 10^{-4}. The electron charge misidentification rate has been measured in $Z/\gamma^* \to e^+e^-$ to be lower than 0.1-0.4% increasing with electron pseudorapidity [25]. We have not applied any correction due to electron charge misidentification once we checked the negligible impact in our signal region. However, we have used the statistical error of the charge misidentification rate [25] as systematic uncertainty. The W^+Z process trends to be produced more boosted than W^-Z due to the energy distribution of the quarks inside the proton. In particular the fraction proton energy probability for the u and $\bar{d}$ quarks pair (W^+Z) is higher than the d, $\bar{u}$ pair (W^-Z), see e.g. Ref. [28]. As a consequence the acceptance for the W^+Z process is expected to be lower than for W^-Z.

The ratio measurement is done by following the selection described in Section 3, adding the requirement to the W candidate lepton to have a positive (negative) charge,

$$N_S^{+(-)} = N_{obs}^{+(-)} - N_{bkg}^{+(-)}$$

Therefore we perform two cross section measurements, one for W^+Z and another for W^-Z.

The same systematic uncertainties as in the inclusive cross section have been considered for the ratio analysis except the luminosity which cancels in the ratio. We have added the statistical uncertainty of the efficiency ratio $\varepsilon^-/\varepsilon^+$, applying a 2.3% variation for each muon and 3% for each electron; and the statistical uncertainty of the electron charge misidentification probability, 0.3%.

Following the same procedure as for the inclusive cross section analysis, the ratio is measured in the four channels considered and the results are reported in Tables 6 and 7 for the 7 and 8 TeV run, respectively.

The BLUE method [22] is used to obtain a combined measurement from the four independent values, with the same error correlations as in the inclusive cross section measurement applied.

Table 6: Measured cross section W^+Z and W^-Z ratio values in the four leptonic channels at 7 TeV.

channel	$\sigma_{W^+Z}/\sigma_{W^-Z}$
eee	1.92 ± 0.52 (stat.) $\pm$ 0.07 (syst.)
eeμ	1.99 ± 0.58 (stat.) $\pm$ 0.04 (syst.)
$\mu\mu$e	2.02 ± 0.58 (stat.) $\pm$ 0.08 (syst.)
$\mu\mu\mu$	1.87 ± 0.40 (stat.) $\pm$ 0.03 (syst.)
combined	1.94 ± 0.25 (stat.) $\pm$ 0.04 (syst.)

Table 7: Measured cross section W^+Z and W^-Z ratio values in the four leptonic channels at 8 TeV.

channel	$\sigma_{W^+Z}/\sigma_{W^-Z}$
eee	1.59 ± 0.24 (stat.) $\pm$ 0.04 (syst.)
eeμ	1.89 ± 0.27 (stat.) $\pm$ 0.04 (syst.)
$\mu\mu$e	2.06 ± 0.26 (stat.) $\pm$ 0.05 (syst.)
$\mu\mu\mu$	1.80 ± 0.19 (stat.) $\pm$ 0.04 (syst.)
combined	1.81 ± 0.12 (stat.) $\pm$ 0.03 (syst.)

The inclusive cross section ratio for $71 < m_Z < 111$ GeV is measured to be

$$\left(\frac{\sigma_{W^+Z}}{\sigma_{W^-Z}}\right)_{7\ \text{TeV}} = 1.94 \pm 0.25\ (\text{stat.}) \pm 0.04\ (\text{syst.})$$

which is in agreement with the SM prediction of $1.776^{+0.006}_{-0.003}$, computed at NLO with MCFM with the MSTW2008 PDF set.

The same ratio at $\sqrt{s} = 8$ TeV is measured to be

$$\left(\frac{\sigma_{W^+Z}}{\sigma_{W^-Z}}\right)_{8\ \text{TeV}} = 1.81 \pm 0.12\ (\text{stat.}) \pm 0.03\ (\text{syst.})$$

which is also in agreement with the SM prediction of 1.724 ± 0.003 computed in the same way.

7 Conclusions

An improved measurement of the WZ cross section at 7 TeV and the first measurement of WZ production with the CMS detector at 8 TeV have been presented, based on data taken in 2011 and 2012, corresponding to an integrated luminosity of 4.9 fb^{-1} at 7 TeV and 19.6 fb^{-1} at 8 TeV. The W and Z bosons are identified through their decays into electrons and muons. The measured value for the WZ production cross section in proton-proton collisions at $\sqrt{s} = 7$ TeV, for $71 < m_Z < 111$ GeV, is

$$\sigma\left(pp \to WZ + X; \sqrt{s} = 7\,\text{TeV}\right) = 20.76 \pm 1.32\ (\text{stat.}) \pm 1.13\ (\text{syst.}) \pm 0.46\ (\text{lumi.})\ \text{pb}$$

while the SM prediction for this cross section is $17.8^{+0.7}_{-0.5}$ pb, computed at NLO with MCFM [23].

The measured value for the same cross section at $\sqrt{s} = 8$ TeV is:

$$\sigma\left(pp \to WZ + X; \sqrt{s} = 8\,\text{TeV}\right) = 24.61 \pm 0.76\ (\text{stat.}) \pm 1.13\ (\text{syst.}) \pm 1.08\ (\text{lumi.})\ \text{pb}$$

The SM prediction, also computed at NLO with MCFM, is $21.91^{+1.17}_{-0.88}$ pb.

The ratio of W^+Z to W^-Z production cross sections has also been measured for proton-proton collisions at $\sqrt{s} = 7\,\text{TeV}$ and $\sqrt{s} = 8\,\text{TeV}$,

$$\left(\frac{\sigma_{W^+Z}}{\sigma_{W^-Z}}\right)_{7\ \text{TeV}} = 1.94 \pm 0.25\ (\text{stat.}) \pm 0.04\ (\text{syst.})$$
$$\left(\frac{\sigma_{W^+Z}}{\sigma_{W^-Z}}\right)_{8\ \text{TeV}} = 1.81 \pm 0.12\ (\text{stat.}) \pm 0.03\ (\text{syst.})$$

The SM prediction for this ratio at $\sqrt{s} = 7$ TeV is $1.776^{+0.006}_{-0.003}$, and 1.724 ± 0.003 at $\sqrt{s} = 8$ TeV.

References

[1] D0 Collaboration, "A measurement of the WZ and ZZ production cross sections using leptonic final states in 8.6 fb^{-1} of $p\bar{p}$ collisions", *Phys.Rev.* **D85** (2012) 112005, doi:10.1103/PhysRevD.85.112005, arXiv:1201.5652.

[2] CDF Collaboration, "Measurement of the WZ Cross Section and Triple Gauge Couplings in $p\bar{p}$ Collisions at $\sqrt{s} = 1.96$ TeV", *Phys.Rev.* **D86** (2012) 031104, doi:10.1103/PhysRevD.86.031104, arXiv:1202.6629.

[3] ATLAS Collaboration, "Measurement of the WZ production cross section and limits on anomalous triple gauge couplings in proton-proton collisions at $\sqrt{s} = 7$ TeV with the ATLAS detector", *Phys. Lett. B* **709** (2012) 341, doi:10.1016/j.physletb.2012.02.053, arXiv:1111.5570.

[4] ATLAS Collaboration, "A Measurement of $W^{\pm}Z$ Production in Proton-Proton Collisions at $\sqrt{s} = 8$ TeV with the ATLAS Detector", *ATLAS Note* **ATLAS-CONF-2013-021** (2013).

[5] CMS Collaboration, "Measurement of the WW, WZ and ZZ cross sections at CMS", Technical Report CMS-PAS-EWK-2011-010, (2011).

[6] CMS Collaboration, "Search for a W' or ρ_{TC} decaying into WZ in pp collisions at $\sqrt{s} = 8$ TeV", CMS Physics Analysis Summary CMS-PAS-EXO-2012-025, (2013).

[7] CMS Collaboration, "The CMS experiment at the CERN LHC", *JINST* **3** (2008) S08004, doi:10.1088/1748-0221/3/08/S08004.

[8] J. Alwall, P. Demin, S. de Visscher, R. Frederix, M. Herquet, F. Maltoni, T. Plehn, D. L. Rainwater, and T. Stelzer, "MadGraph/MadEvent v4: the new web generation", *JHEP* **09** (2007) 028, doi:10.1088/1126-6708/2007/09/028.

[9] S. Frixione, P. Nason, and C. Oleari, "Matching NLO QCD computations with parton shower simulations: the POWHEG method", *JHEP* **11** (2007) 070, doi:10.1088/1126-6708/2007/11/070.

[10] H.-L. Lai et al., "Uncertainty induced by QCD coupling in the CTEQ-TEA global analysis of parton distributions", arXiv:1004.4624.

[11] H.-L. Lai et al., "New parton distributions for collider physics", *Phys. Rev.* **D82** (2010) 074024, doi:10.1103/PhysRevD.82.074024, arXiv:1007.2241.

[12] GEANT4 Collaboration, "GEANT4: A Simulation toolkit", *Nucl. Instrum. Meth.* **A506** (2003) 250–303, doi:10.1016/S0168-9002(03)01368-8.

[13] CMS Collaboration, "Performance of muon identification in pp collisions at $\sqrt{s} = 7$ TeV", Technical Report CMS-PAS-MUO-10-002, (2010).

[14] CMS Collaboration, "Measurement of W^+W^- Production and Search for the Higgs Boson in pp Collisions at $\sqrt{s} = 7$ TeV", *Phys. Lett. B* **699** (2011) 25–47, doi:10.1016/j.physletb.2011.03.056, arXiv:1102.5429.

[15] CMS Collaboration, "Electron Reconstruction and Identification at $\sqrt{s} = 7$ TeV", Technical Report CMS-PAS-EGM-10-004, (2010).

[16] CMS Collaboration, "Particle Flow Event Reconstruction in CMS and Performance for Jets, Taus, and MET", Technical Report CMS-PAS-PFT-09-001, (2009).

[17] CMS Collaboration, "Measurements of Inclusive W and Z Cross Sections in pp Collisions at $\sqrt{s} = 7$ TeV", *JHEP* **01** (2011) 080, doi:10.1007/JHEP01(2011)080, arXiv:1012.2466.

[18] CMS Collaboration, "Commissioning of the particle-flow event reconstruction with leptons from J/ψ and W decays at 7 TeV", Technical Report CMS-PAS-PFT-10-003, (2010).

[19] CMS Collaboration, "Measurement of the ZZ production cross section and search for anomalous couplings in 2 l2l ′ final states in pp collisions at $\sqrt{s} = 7$ TeV", *JHEP* **1301** (2013) 063, doi:10.1007/JHEP01(2013)063, arXiv:1211.4890.

[20] CMS Collaboration, "Measurement of W^+W^- and ZZ production cross sections in pp collisions at $\sqrt{s} = 8$ TeV", *Phys.Lett.* **B721** (2013) 190–211, doi:10.1016/j.physletb.2013.03.027, arXiv:1301.4698.

[21] CMS Collaboration, "Measurement of the Wγ and Zγ Cross Sections and Limits on Anomalous Triple Gauge Couplings at $\sqrt{s} = 7$ TeV", CMS Physics Analysis Summary CMS-PAS-EWK-2011-009, (2011).

[22] L. Lyons, D. Gibaut, and P. Clifford, "How to combine correlated estimates of a single physical quantity", *Nucl.Instrum.Meth.* **A270** (1988) 110, doi:10.1016/0168-9002(88)90018-6.

[23] J. M. Campbell and R. K. Ellis, "MCFM for the Tevatron and the LHC", *Nucl. Phys. Proc. Suppl.* **205** (2010) 10, doi:10.1016/j.nuclphysbps.2010.08.011, arXiv:1007.3492.

[24] A. Martin, W. Stirling, R. Thorne, and G. Watt, "Parton distributions for the LHC", *Eur. Phys. J. C* **63** (2009) 189–285, doi:10.1140/epjc/s10052-009-1072-5, arXiv:0901.0002.

[25] CMS Collaboration, "Measurement of the Electron Charge Asymmetry in Inclusive W production in pp collisions at $\sqrt{s} = 7$ TeV", *Phys. Rev. Lett.* **109** (2012) 111806, doi:10.1103/PhysRevLett.109.111806, arXiv:1206.2598.

[26] CMS Collaboration, "Measurement of the Muon Charge Asymmetry in Inclusive W production in pp Collisions at $\sqrt{s} = 7$ TeV", CMS Physics Analysis Summary CMS-PAS-EWK-2011-005, (2011).

[27] CMS Collaboration, "Measurement of the charge ratio of atmospheric muons with the CMS detector", *Phys.Lett.* **B692** (2010) 83–104, doi:10.1016/j.physletb.2010.07.033, arXiv:1005.5332.

[28] P. M. Nadolsky et al., "Implications of CTEQ global analysis for collider observables", *Phys.Rev.* **D78** (2008) 013004, doi:10.1103/PhysRevD.78.013004, arXiv:0802.0007.